AFRL-OSR-VA-TR-2013-0513

INTEGRATED PLASMONIC NANOCIRCUITS

MARK BRONGERSMA

LELAND STANFORD JUNIOR UNIVERSITY

09/23/2013
Final Report

DISTRIBUTION A: Distribution approved for public release.

AIR FORCE RESEARCH LABORATORY
AF OFFICE OF SCIENTIFIC RESEARCH (AFOSR)/RSE
ARLINGTON, VIRGINIA 22203
AIR FORCE MATERIEL COMMAND

REPORT DOCUMENTATION PAGE

Form Approved
OMB No. 0704-0188

1. REPORT DATE *(DD-MM-YYYY)*
9-4-2013

2. REPORT TYPE
Final Performance Report

3. DATES COVERED *(From - To)*
13/05/2010 - 14/05/2013

4. TITLE AND SUBTITLE
Integrated Plasmonic Nanocircuits

5a. CONTRACT NUMBER
N/A

5b. GRANT NUMBER
FA9550-10-1-0264

5c. PROGRAM ELEMENT NUMBER

6. AUTHOR(S)
Brongersma, Mark

5d. PROJECT NUMBER

5e. TASK NUMBER

5f. WORK UNIT NUMBER

7. PERFORMING ORGANIZATION NAME(S) AND ADDRESS(ES)
Leland Stanford University
Office of Sponsored Research
651 Serra Street, Room 260
Stanford, CA 94305-4125

8. PERFORMING ORGANIZATION REPORT NUMBER
SPO # 49734

9. SPONSORING/MONITORING AGENCY NAME(S) AND ADDRESS(ES)
Dr. Gernot Pomrenke
Air Force Office of Scientific Research
875 N. Randolph St.
Ste 325, Room 3112
Arlington, VA 22203-1768

10. SPONSOR/MONITOR'S ACRONYM(S)
AFOSR

11. SPONSOR/MONITOR'S REPORT NUMBER(S)

12. DISTRIBUTION/AVAILABILITY STATEMENT
Approved for public release; distribution is unlimited.

13. SUPPLEMENTARY NOTES

14. ABSTRACT
This is the final performance report for a program entitled: "Integrated Plasmonic Nanocircuits". The proposed effort aimed to develop nanoscale optoelectronic nanocircuit elements capable of converting electrical signals to optical signals and back. As part of the program, we developed some of the smallest optical sources and detectors to date. We also demonstrated that new functionalities can be obtained by bringing resonant metallic and semiconductor nanostructures together in optoelectronic devices. In such devices, the constituent materials perform simultaneous electronic and optical functions. This type of multi-functional devices allow for denser integration on a chip. The fabricated structures can find direct application in integrated biosensors and quantum optics experiments. Longer term, the constituent hybrid nanophotonics devices will find their way into a variety of communication, security, and computing systems that are critical to the DoD. In these systems they can serve as an efficient bridge between nanoscale electronic components and (diffraction-limited) dielectric photonics.

15. SUBJECT TERMS
Integrated subwavelength optical sources, nanoscale photodetectors, non-linear optics, FDFD simulation tools, optical cloaking, optical antennas and cavities, cathodoluminescence.

16. SECURITY CLASSIFICATION OF: a. REPORT	b. ABSTRACT	c. THIS PAGE	17. LIMITATION OF ABSTRACT	18. NUMBER OF PAGES	19a. NAME OF RESPONSIBLE PERSON
U	U	U			Cynthia Sanchez
					19b. TELEPHONE NUMBER *(Include area code)* (650) 725-4329

Reset

Final Performance Report

AFOSR Grant Number FA9550-10-1-0264
13 June 2010 – 14 June 2013

Descriptive Title: "Integrated Plasmonic Nanocircuits"

Grantee Institution: **Stanford University**
476 Lomita Mall
Stanford, CA 94305

Program Manager: **Dr. Gernot Pomrenke,**
Tel: (703) 696-8426
Email: gernot.pomrenke@afosr.af.mil

Principal Investigator: **Dr. Mark L. Brongersma**
Tel: (650) 736 2152
Email: Brongersma@stanford.edu

Table of Contents

I. Executive summary

I.1. Statement of Objectives and key accomplishments

Future military systems will utilize highly sophisticated electronic, photonic, and wireless networks to connect tactical forces with command and control. This research program established a coherent research effort on the largely unexplored field of *hybrid nanophotonic* devices that can add new capabilities to such networks. Such devices bring together nanoscale metallic (i.e. plasmonic) and semiconductor components in new and creative ways to enhance each other's function. They effectively capitalize on strengths of plasmonic structures (manipulation of light at the nanoscale) and semiconductor nanostructures (logic functions and interconversion between photons into electrons). The unique physical properties of the different constituent materials in a hybrid nanophotonic device can be leveraged to enable unparalleled integration densities and add valuable functionality to existing electronic and photonic components. Whereas individual nanophotonic building blocks for the generation, modulation, and detection of light and surface plasmons have already been demonstrated, their efficiencies and integration with electronics and dielectric photonics still needs significant work.

In this program, we developed nanoscale optical sources and detectors that are tightly integrated with electronics and can readily be inserted into nanoscale optoelectronic circuits. Such circuits can find direct application in integrated biosensors and quantum optics experiments. Longer term, the constituent hybrid nanophotonics devices will find their way into a variety of communication, security, and computing systems that are critical to the DoD. In these systems they will serve as an efficient bridge between nanoscale electronic components and (diffraction-limited) dielectric photonics. We aimed to show that a tremendous synergy can be attained by seamlessly integrating hybrid nanophotonic, electronic, and conventional photonic components and by having the constituent materials perform simultaneous electronic and optical functions. The key accomplishment of this effort are:

- Created new chipscale optoelectronic device in which the metals and semiconductors perform simultaneous electronic and optical functions. The devices included nanoscale optical sources and photodectors that offer unique new functionalities such as angular emission control, active emission wavelength control, and invisibility.
- Development of new computational tools for analyzing the powerflow 1) from quantum emitters 2) via optical antennas 3) into optical waveguides or free-space.
- Further developed electron-beam based techniques to analyze materials and optical properties at the nanoscale. In particular we used cathodoluminescence in a scanning electron microscope to link the structural properties and optical properties of nanoscale metallic cavities.
- The research from this 3-year program led to a 2 book chapters and a total of 7 publications in refereed journals of which there were a number in very prestigious journals such as Nature Photonics, Nature Communications, and Science.
- Knowledge transfer to Ultimara on beamsteering devices and to Intel on nanoscale optical sources.

I.2. Impact and Relevance of the Effort

The development of the transistor and integrated circuit has led to remarkable electronic data processing capabilities that permeate almost every facet of our daily lives. Optical interconnects with their overwhelming information carrying capacity have become the dominant means for long haul, local area, and in-building information exchange in modern society. Current scaling trends in the microelectronics and communication industry indicate that the dimensions of electronic and photonic devices are rapidly approaching the nanoscale. For future active electronic devices, scaling problems with electronic interconnection become increasingly daunting. The design of photonic structures was running into a seemingly unsurpassable obstacle: The diffraction limit.

Surface plasmon-polaritons (SPP) are easily accessible excitations, whose unique physical properties are now enabling an entirely new class of nanophotonic circuits operating on a scale far below the optical wavelength. The Brongersma group executed a coherent effort to develop nanoscale sources and detectors with underlying electronics and to obtain new functionality that cannot be obtained in any other way. In addition to the development of new device technologies, the team made significant contributions to the development of new simulation tools (calculations of powerflow from emitters and the local density of optical states in nanoscale cavities), optical analysis tools to aid the design of nanoscale optical sources, antennas, and cavities (cathodoluminescence) and made new fundamental science discoveries (e.g. plasmonic enhanced electric field induced second harmonic generation, antenna-electrodes capable of simultaneously injecting charge and manipulating light, and invisible photodetectors) in the now thriving field of nanophotonics. This knowledge has been transferred during a large number of invited presentations and started new interactions with two companies (Intel and Ultimara).

II. Research Accomplishments

II.1. New tool to follow the flow of light from quantum emitters

In the design of nanoscale optical sources, it is critical to understand, optimize, and control the light extraction from quantum emitters into an optical waveguide or to free-space. Current methods to calculate the emission enhancement of a quantum emitter coupled to an optical antenna or nanoscale cavity of arbitrary geometry rely on analyzing the *total* Poynting vector power flow out of the emitter or the dyadic Green functions from full-field numerical simulations. Unfortunately, these methods do not provide any information regarding the nature of the dominant energy decay pathways. In this project we developed a new approach to this problem that allows for a rigorous separation, quantification, and visualization of the emitter output power flow captured by an antenna or cavity and the subsequent reradiation power flow from the structure to a waveguided mode or to the far-field.

As an example, Figure 1 show how a quantum emitter optically couples to a metallic strip antenna (white). Figure 1a visualizes the powerflow out of the emitter directly into free-space (blue flow-lines) and into the antenna (red flow-lines). Fig 1b shows how some of the power that was initially transferred from the emitter to the antenna can be reradiated into free space. This reradiated powerflow has an angular and polarization distribution that is controlled by the antenna geometry. In this case we designed a dipolar antenna that reradiates energy in a simple dipolar emission distribution.

This developed powerflow analysis enables one to optimize the transfer of optical (i.e. "light") energy from the emitter to the antenna. It can then be used to effectively control emission properties (e.g. spectral, angular, polarization) from the quantum emitter by smart antenna design. This type of analysis has revealed unprecedented details of the emitter/antenna coupling mechanisms and opened up new design strategies for strongly interacting emitter/ antenna systems used in sensing, active plasmonics and metamaterials, and quantum optics. The work was published in Optics Express (Kevin C. Y. Huang et al., Optics Express, 19, 19084-19092, 2011).

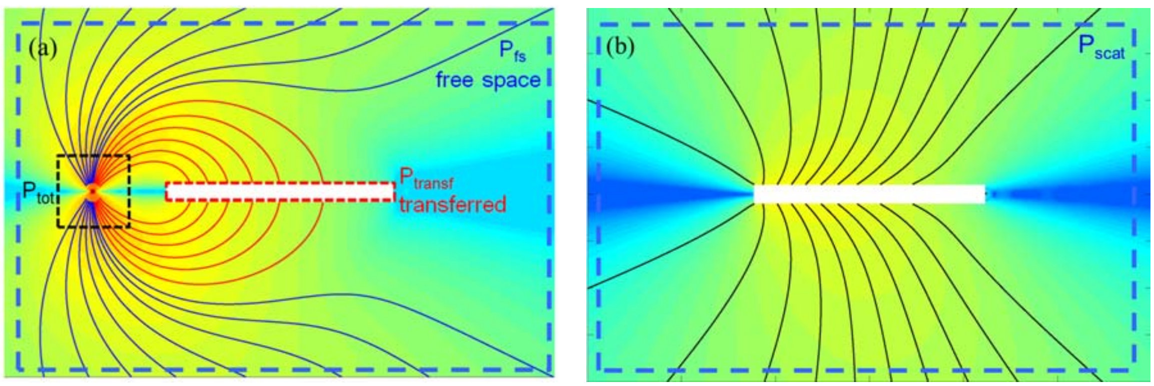

Figure 1. Visualizations of the emission from a horizontally-oriented quantum emitter placed in proximity of a metallic stripe antenna (white). (a) shows the powerflow from the emitter directly to the far-field in blue and into the antenna in red. (b) shows how a fraction of the power that was transfer to the antenna is reradiated with an angular distribution that is controlled by the antenna's geometry.

II.2. Plasmonic beaming and active emission control

Nanometallic optical antennas are rapidly gaining popularity in applications that require exquisite control over light concentration and emission processes. As part of our effort on plasmonic nanocircuits, we aimed we aimed to develop optical antennas that offer facile integration on chips. In our project, we demonstrate a new, easily-fabricated optical antenna design that achieves an unprecedented level of control over fluorescent emission by combining concepts from plasmonics, radiative decay engineering, and optical beaming. The antenna consists of a nanoscale plasmonic cavity filled with quantum dots (QDs) coupled to a miniature grating structure that can be engineered to produce one or more highly collimated beams. We used the simulation approach described in section II.1. to design the antenna structures and applied confocal microscopy to visualize the beaming process. We also showed that the metals defining the plasmonic cavity can be utilized to electrically control the emission intensity and wavelength. This fits in within the theme of our proposed effort to develop plasmonic devices in which the metals and semiconductors can perform simultaneous electronic and optical functions.

Figure 2a shows confocal microscopy images that visualize the flow of light out of our nanoscale antenna structures into the far-field. The figure shows that the emission from QDs placed inside a slit without side grooves is diffracted into a broad range of angles, as expected for the emission from a subwavelength aperture. However, Fig. 2b shows that a collimated beam can be produced by choosing optimized groove parameters. This geometrical optimization ensures that the planar SPPs launched from the slit decouple with the right phases to produce a narrow central beam via constructive interference. Furthermore, the structure effectively suppresses the formation of emission side lobes. Figure 2c shows the off-axis collimation of the QD emission using an asymmetric slit-groove structure. We achieved unprecedentedly small divergence angles of 11.5° and 11.3° for the symmetric and asymmetric slit-groove structures respectively. Vertical collimation of the QD emission was also verified by direct Fourier plane imaging. For all of the antenna structures a substantial decrease in the QD emission lifetime was observed as compared to QDs placed on a quartz substrate (Purcell effect) and it was found that the change in lifetime was strongly correlated to the central slit width.

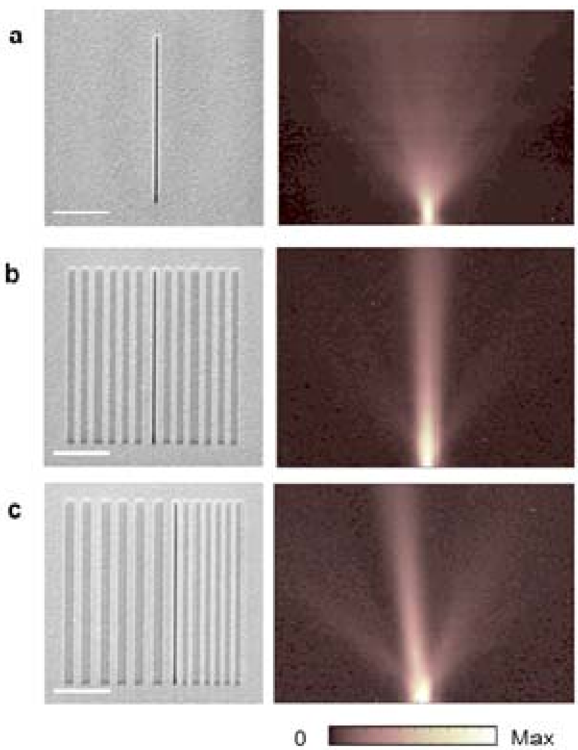

Figure 2. SEM images of several plasmonic antennas and corresponding XZ confocal scanning images of the quantum dot emission. a, An 80-nm-wide slit in a metal film that is filled with CdSe quantum dots (QDs) (left). A confocal optical image visualizing the flow of light from the QD emitters out of the slit into the far-field. The image shows that the light from the subwavelength slit quickly diffracts to produce a highly-divergent beam. b, An 80-nm-wide slit filled with QDs, but now with a set of side-grooves optimized to produce a collimated beam normal to the metal surface (left). Confocal image of the collimated light-emission from the antenna structure (right) c, An asymmetric slit-groove structure optimized to produce an angled beam (Left).Confocal image showing the angled emission from the antenna. Scanning area is 20 µm in x-direction and 15 µm in the z-direction. The white scale bar in the SEM image is 2 µm.

As part of this work, we also demonstrated the ability to tune the emission spectrum from the QDs by applying a voltage across the slit. A spectral red-shift was observed upon application of the voltage. The quadratic shift in the emission wavelength with applied voltage is as expected for the Quantum Confined Stark effect. These findings facilitate the realization of a new class of active optical antennas for use in novel optical sources and a wide range of nanoscale optical spectroscopy applications. The work was published in Nature Communications ("Plasmonic beaming and active control over fluorescent emission," Young Chul Jun, Kevin C.Y. Huang, and Mark L. Brongersma, Nature Communications, 2, 283, 2011).

II.3. Electrically Controlled Non-linear Generation

In our research under this program, we demonstrated that plasmonics offers a tantalizing opportunity to develop ultra-compact optical devices on a chip by capitalizing on two of its most important strengths: extreme light concentration to far below the diffraction limit and an ability to perform simultaneous electrical and optical functions. These strengths also make plasmonics an ideal candidate for dynamically controlling nonlinear optical interactions at the nanoscale, an area that has remained unexplored. Following our work on plasmonic beaming, we managed to experimentally demonstrate electrically-tunable harmonic generation of light from a plasmonic nanocavity filled with a nonlinear medium (see Figure 3). For this we essentially used the same structure as shown in Figure 2b. The metals that define the cavity also serve as electrodes that can generate high DC electric fields across the nonlinear material. With this electric field, we were able to tune the frequency-doubling of a 1.56 μm fundamental wave. A moderate external voltage to the electrodes, yielded a nonlinear modulation magnitude of ~7% per volt and ~140% at a bias voltage of 20 V. This high-impact work was published in Science ("Electrically Controlled Nonlinear Generation of Light with Plasmonics," Wenshan Cai, Alok P. Vasudev, Mark L. Brongersma, Science 333, 1720-1723, 2011.

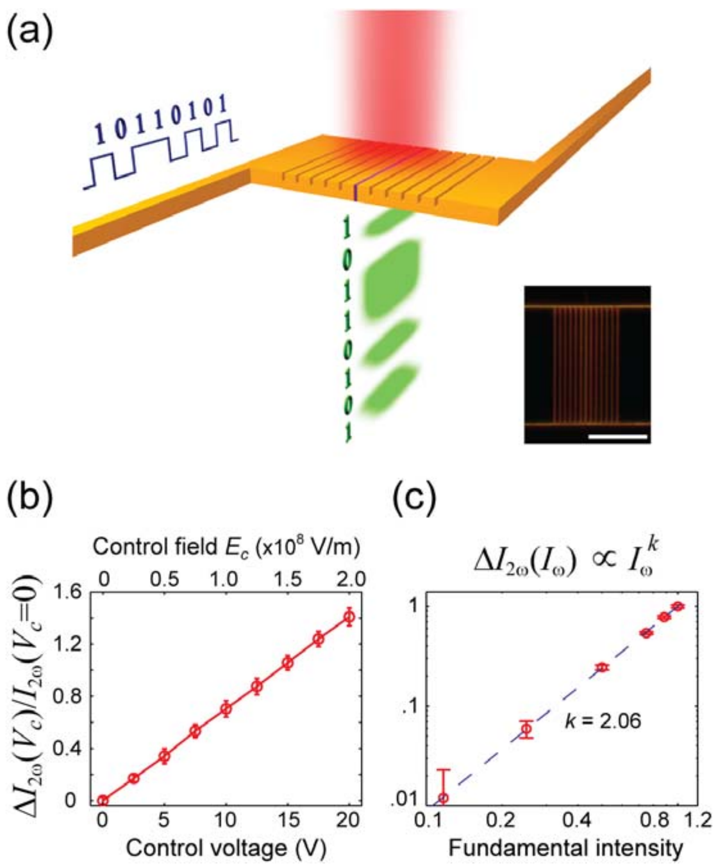

Figure 3. Electrical control of second harmonic generation with plasmonics. (a) Schematic of the nonlinear device where a plasmonic nanocavity contains a commonly used polymer poly(methyl methacrylate). In the room-temperature experiment, the fundamental wave at ~1.5 μm illuminated the metallic structure from the top. The inset shows a dark-field optical microscope image with a scale bar of 10 μm. (b) The normalized change in the frequency-doubled output as a function of the control voltage. Error bars represent standard deviations from five measurements. A nonlinear modulation depth of 140% is observed at an external bias of 20 V. (c) The dependence of the voltage-induced harmonic output on the intensity of the fundamental light. The dashed line represents least-squares fit indicating a slope of 2.06.

II.4. An "Invisible" Photodetector

On the detection side, we have worked on nanoscale photodetectors that feature enhanced performance over their larger counterparts and ones with entirely new functionalities. One of our goals in this program was to realize a new class of chipscale devices that not only exploits the unique *material*-dependent properties of semiconductors and metals, but also capitalizes on the notion that nanostructures of these materials exhibit strong and tunable optical responses that critically depend on their *geometry* and *size*. The realization of such device requires a new design methodology in which the geometrical properties of the constituent building blocks have to be carefully tuned in conjunction with their materials properties. As the electronic side of such optimizations is well-understood, we focused on developing systematic optical optimization. In this optimization, one first selects subwavelength building blocks based on desired electrical and optical materials properties. In a second step, the limited number of optical resonances of the building blocks are identified as well as their tunability with size, shape and dielectric environment. In a third step, the building blocks are assembled in a subwavelength region and one or more desired optical functions are realized by capitalizing on strong modal hybridization and intermodal interference effects between these small objects. This procedure typically has a number of constraints that are set forth by electronic requirements (e.g. electrical connectivity). In this delicate *harmonization* process, the optimization of specific geometries and sizes in fact becomes as important as the materials selection. In the resulting photodetector, the constituent semiconductors and metals naturally play an electronic (charge extraction) and optical (cloaking) function *at the same time and in the same physical space*. Moreover, the traditional spatial boundaries between electronic and photonic components have disappeared and new opportunities for ultra-dense integration emerge. Here we applied our optimization/harmonization procedure to develop an invisible photodetector.

Figure 4a shows a schematic of the photodetector we realized with metallic contacts overcoating a semiconductor nanowire. Its design started with a materials selection based on desired electrical and optical properties. We chose a Si nanowire for its excellent electronic transport properties and its ability to transduce light to photocurrent. We chose to place a high electrical conductivity metal (Au) contact on top of the wire to enable efficient charge extraction. From an optical perspective, it is not intuitively clear whether coating the nanowire with a reflective metal would be beneficial. However, we showed that the geometrical properties of the metallic contacts and the semiconductor nanowire can be re-engineered to perform several valuable optical functions, including the first experimental demonstration of a cloaking sensor in the visible part of the electromagnetic spectrum.

In the second design step, we considered the optical modes of the metal contact and the high refractive index Si nanowires. The optical properties of metal nanostructures are by now quite well-established. These negative dielectric constant (ε) objects support surface plasmon (SP) resonances which are collective oscillations of free electrons that couple to electromagnetic fields. In order to build a device capable of producing photocurrent, it is essential to introduce semiconductors and to hide it from the eye we need both the metal and semiconductor components to exhibit optical resonances. Here, we employed a strongly geometry-dependent optical (Mie) resonance that naturally occurs in high-dielectric-constant semiconductor nanostructures. Interestingly, they can occur in deep-subwavelength structures (~ 10 nm), as small as state-of-the-art electronic components. Here, we aim to join geometrically-resonant metallic and semiconductor nanostructures together into highly functional hybrid devices that derive their properties from their near-field coupling and intermodal interference.

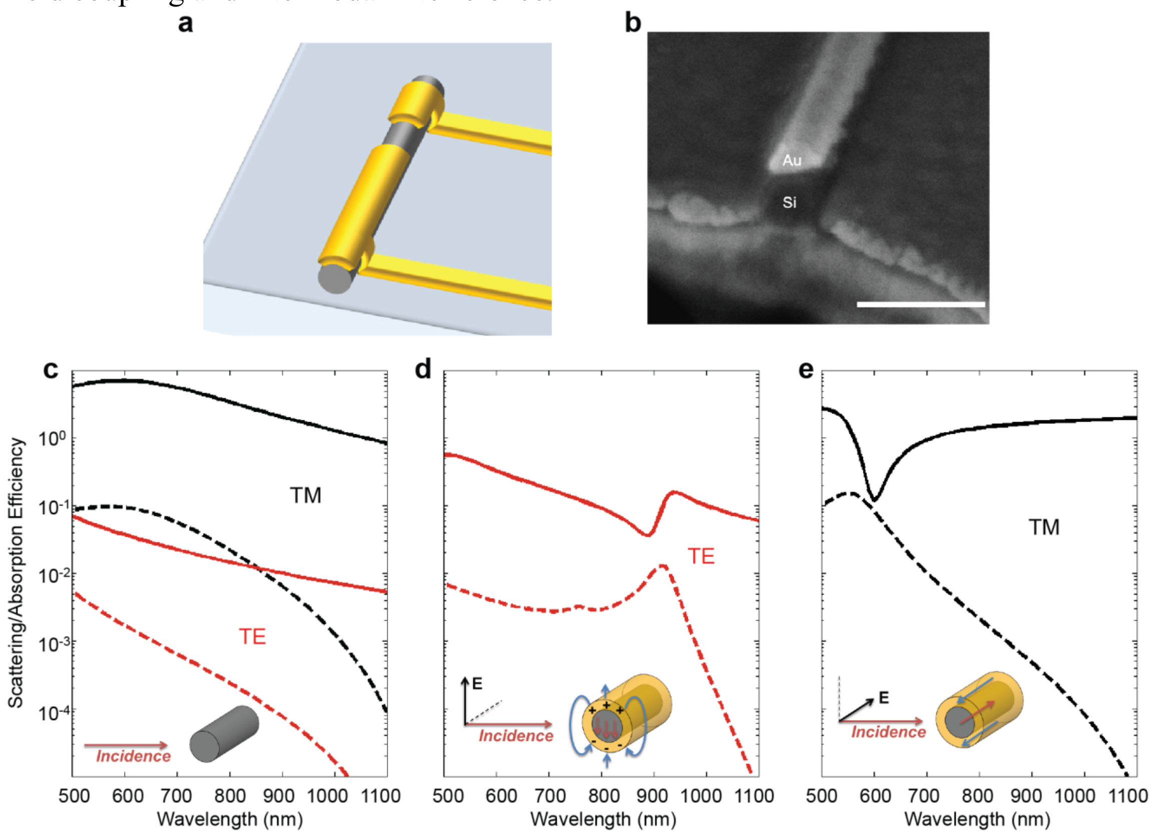

Figure 4. Design and operation of a hybrid Au/Si nanowire photodetector. a. Schematic of a Si nanowire (grey) photodetector hooked up by two Au electrodes (yellow) which are used for photocurrent extraction. b. Scanning electron microscopy image of a 50-nm-diameter Si nanowire with a 20-nm-thick Au "cover". Scale bar is 100 nm. c. Scattering (solid curves) and absorption (dashed curves) cross sections as a function of wavelength for a 50-nm-diameter Si nanowire. The scattering and absorption are much stronger under transverse magnetic (TM) illumination (black curves) than under transverse electric (TE) illumination (red curves) due to the presence of a strong optical TM resonance near 600 nm. It can also be seen that scattering dominates absorption for both polarizations. d. The scattering and absorption cross sections for the same Si nanowire as in 1c, but now with a 15-nm-thick, Au shell under TE illumination. For TE illumination, a surface plasmon resonance can be driven in the Au shell, as illustrated in the inset. As a result, scattering and absorption are greatly enhanced in the hybrid structure. The peak around 900nm in the Si absorption is attributed to a dipolar surface plasmon resonance. e. For TM illumination, the Si core and Au shell are polarized in opposite directions and this gives rise to a dramatic reduction in the scattering efficiency of the hybrid structure; in practical terms, the wire becomes invisible or "cloaked" near 600 nm and the absorption efficiency at this wavelength dominates the scattering.

Figure 4b shows a cross-section scanning electron microscopy (SEM) image of our fabricated hybrid nanowire photodetector consisting of a 50-nm-diameter Si nanowire with a 20-nm-thick gold cover. Spectral light scattering and photocurrent experiments on this type of structure were performed and described in a paper listed below. In this report, we primarily focus on the design and essential physics behind the unique properties of the device.

In the third design step, we explored how the optical response of the hybrid semiconductor/metal structure could be tailored by engineering the interaction between the modes of the Si nanowire and Au contact. The possible interactions were first examined in two idealized model systems: a bare Si nanowire and a Si nanowire with a concentric Au shell (insets to Figs 4c-e). The optical response of these structures is strongly polarization-dependent. For top-illuminated cylinders, the optical modes can be divided into transverse-magnetic (TM, with the electric field along the axis of the nanowire) and transverse-electric (TE, with the electric field normal to the axis of the nanowire) modes. The scattering and absorption efficiencies of the different wires were calculated as a function of wavelength for both polarizations using the Mie theory. In these calculations shown in Figs 1c-e, only light absorption inside the Si wire is included as its magnitude determines the number of photocarriers that could be extracted from a nanowire detector. Figure 4c shows the scattering (solid curves) and absorption (dashed curves) efficiencies of the bare Si nanowire for TM (black) and TE (red) illumination. The spectral region of interest from 500 nm – 1100 nm shows a strong lowest-order, monopolar TM_{01} resonance in the scattering and absorption that is peaked near 620 nm. The subscripts refers to the azimuthal mode number (m = 0), which indicates an effective number of wavelengths around the wire circumference and the radial order number (l = l), describing the number of radial field maxima within the cylinder. Physically, the excitation of this mode corresponds to a displacement current that is driven back and forth along the wire axis with a maximum in the core of the wire. Under TE illumination, both the scattering and absorption are much weaker and exhibit a monotonic decay with increasing wavelength. This is explained by the absence of TE resonances in this spectral region. For both polarizations, light scattering form the nanowire dominates the absorption inside the semiconductor. This is a direct consequence of the relatively weak materials absorption of indirect-gap, crystalline Si in this wavelength range.

Figures 4d and e show that the addition of an Au shell dramatically alters the optical response of the Si nanowire for both TE and TM illumination. The inset to Fig. 4d shows how a particle-like surface plasmon resonance can be driven in the Au shell under TE illumination. The excitation of SPs produces high fields inside the Si wire. As such, the shell effectively serves as an optical antenna capable of concentrating light into the wire and enhancing the photoresponse. A significant plasmonic enhancement in the photoresponse is seen at a wavelength near 900 nm; Due to a dipolar resonance in the Au shell, both the scattering by the hybrid wire and the absorption inside the Si are peaked around this wavelength. Figure 4e shows that the scattering efficiency under TM illumination is of a similar magnitude as the bare nanowire near 500 nm and 1100 nm. However, near 600 nm a 2-orders-of-magnitude reduction in the scattering efficiency is observed. This effect is explained by realizing that under TM illumination both the wire and Au cover are strongly polarized along the wire axis. In this example, the shell thickness was carefully chosen such that incident light at 600 nm induces an electric dipole moment in the shell that is equal in magnitude but opposite in sign to the dipole moment in the wire. This results in a net zero total electric dipole moment in the combined wire/shell system. The deep-subwavelength size of the hybrid-wire cross section ensures that the opposing dipoles cancel each other's scattering in the far-field. This phenomenon is known as plasmonic cloaking. Although the net dipole moment of the coated wire is zero, the dipole moment in the Si wire can be large and implies that photocarriers are generated.

The results of this study demonstrate the critical importance of performing a joint optimization of the electrical and optical properties of the metallic and semiconductor building blocks in optoelectronic devices with nanoscale components. With the rapid scaling of such components these types of joint optimizations will become increasingly important. Based on its general importance, a paper on this unique photodetector with Nader Engheta's group was published in a high impact journal ("An Invisible Metal-Semiconductor Photodetector," Pengyu Fan, Uday Chettiar, Linyou Cao, Farzaneh Afshinmanesh, Nader Engheta, and Mark L. Brongersma, Nature Photonics 6, 380–385 2012).

II.5 Redesigning Photodetector Electrodes as an Optical Antenna.

Photodetectors play a critical role in many optoelectronic applications, including optical interconnection and imaging. Scaling of these devices has brought many advantages in terms of their operating speed, signal-to-noise ratio, and power consumption. Prior to the start of this program, our group developed highly-efficient photodetectors based on semiconductor nanowires (Si and Ge). At first sight, it appears that scaling of such photodetectors below the diffraction limit would also result in the undesired situation where a detector becomes incapable of capturing all incident photons from an optical beam or waveguide. To overcome this challenge, researchers have successfully employed the light concentrating properties of metallic nanostructures that support surface plasmon excitations. More recently, it has also been shown that the optical Mie resonances that naturally occur in high-dielectric-constant semiconductor nanostructures can be used to boost light absorption in photodetectors and solar cells. In section II.4, we showed that the resonances in metallic and semiconductor nanostructures can even be combined to even further boost device performance or to add entirely new functions such as invisibility. In our program, we next demonstrated that the metallic leads to a nanoscale semiconductor photodetector can be re-engineered to perform simultaneous charge extraction and optical antenna functions. This was illustrated with a metal-semiconductor-metal (MSM) photodetector consisting of a Ge NW placed between two metallic contacts. MSM photodetectors are known for their high speed and low-noise operation.

Figure 5a and 5b illustrate the two most basic configurations in which a Ge nanowire can be contacted to realize a MSM photodetector. The NW (grey) can be positioned either perpendicular or parallel to the gap formed between two metallic contacts (orange). From an electronics viewpoint, it is clearly beneficial to bring the metallic electrodes closer together. Experience with scaling of electronic devices has taught us how a reduction in device footprint comes with the benefits of lower power consumption, a higher signal-to-noise, and an increased speed of operation. From an optical perspective, the benefit of having closely-spaced electrodes made from optically lossy and reflective metals is less obvious as they may partially block or absorb an incident light beam. However, in this project we demonstrated that the narrow, finite-length slit that naturally forms between two closely-spaced metallic electrodes can support strong standing wave resonances of surface plasmon-polaritons (SPPs). When such a resonance is excited, one can capitalize on the high field intensities that build up in the slit to enhance light absorption in a semiconductor medium placed inside the slit. The high refractive index NW in the gap also supports strong optical resonances and with proper engineering it is possible to cascade a semiconductor NW resonance with the metallic slit resonance. In the overall optimization one needs to be cognizant of the fact that both types of resonances are strongly dependent on the size and geometry of the structures as well as the state of polarization of the incident light. In a paper published in Nano Letters ("Redesigning Photodetector Electrodes as an Optical Antenna," Pengyu Fan, Kevin C. Y. Huang, Linyou Cao, and Mark L. Brongersma, Nano Lett., 13, 392–396, 2013) we discussed our design strategy for ultra-compact NW photodetector that was aimed at a joint optimization of the absorbing semiconductor medium and the electrical leads. In the study, we considered two basic device configurations where the Ge NW is either parallel or orthogonal to the slit, as shown in Figure 5a,b and one configuration is discussed briefly below.

To illustrate our line of research in this report, we discuss the case where a Ge NW is placed inside and along the length of the slit formed between two closely-spaced silver (Ag) pads. Figure 5c shows a cross-sectional scanning electron microscopy (SEM) image of this basic configuration. The geometrical parameters of this device were chosen to optimize the light absorption at a (somewhat arbitrarily chosen) target wavelength of 650 nm. To maximize the light absorption at this wavelength, one needs to first select a Ge NW diameter that produces a strong optical resonance at this wavelength. For top-illuminated NWs, the resonant modes can be divided into transverse-magnetic (TM, with the electric field along the axis of the nanowire) and transverse-electric (TE, with the electric field normal to the axis of the nanowire) modes. In deciding whether to select a NW that features a TM or TE resonance, it is important to realize that a plasmonic mode in a metallic slit can only be excited when the electric field is orthogonal to the slit (and thus also orthogonal to the wire in the slit). With the aim to ultimately cascade the NW and slit resonances in the back of our mind, we choose a 90-nm-diameter Ge NW that exhibits the lowest order TE resonance at 650 nm.

After having chosen a NW, we can turn our attention to the optimization of the metallic electrodes. Here, the goal is to effectively drive the standing wave SPP resonances in the slit that result from SPP reflections at the top (entrance) and bottom (exit) of the slit. The spectral location of these resonances is effectively controlled by the length of the slit, i.e. the thickness of the metallic electrodes. Fig 5d shows the simulated dependence of the light absorption in the Ge NW as a function of the thickness of the adjacent Ag pads and a pad-spacing of 150 nm. It can be seen that the magnitude of the NW absorption oscillates with the Ag thickness and shows maxima near 150 nm and 350 nm. The highest peak is near 150 nm, where the NW absorption is increased by as much as 1.9 times over the bare Ge NW. This governed our choice of the metal thickness for the fabricated NW detector structure shown in Fig.5b. To gain physical insight into the nature of the absorption enhancements, we also plot the distribution of the magnetic field intensity H_z in the device cross sections for two optimal thicknesses. For both the 150 nm (Figure 5e) and 350 nm (Figure 5f) thick Ag pads the Ge NW core features a single broad maximum in the H_z intensity, indicating the excitation of the lowest order TE resonance in the NW. Depending on the thickness, one (Figure 5e) or two (Figure 5f) anti-nodes in the H_z intensity could be identified inside the Ag slit. This is consistent with the first and second order standing wave SPP resonances supported in the Ag slits respectively. From these results, it can be concluded that a slit resonance between metallic electrodes can effectively be cascaded with a semiconductor NW resonance to boost the absorption of light beyond what is feasible in the NW by itself. In the Nano Letters listed above, we performed a detailed experimental verification of this type detector.

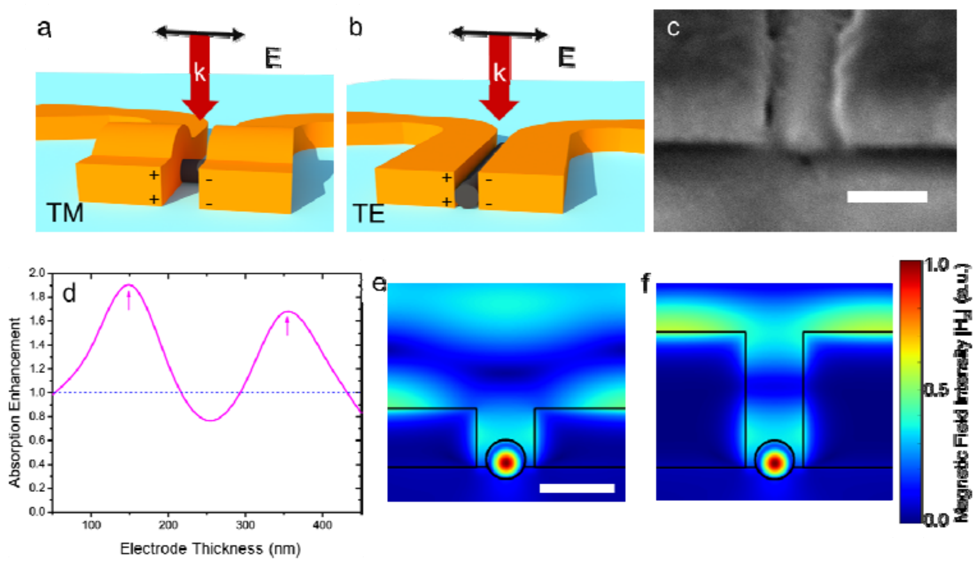

Figure 5. Design of semiconductor nanowire (NW) photodetectors that exploit optical resonances in both the NW itself and the narrow gap formed between the metallic contacts. Metallic contacts in a metal-semiconductor-metal photodetector with a semiconductor NW can be redesigned to act as optical antennas capable of enhancing the optical response. Two basic configurations are explored where the NW is either a) perpendicular or b) parallel to the gap formed between the metallic leads. The image also shows the direction of the electric field for the case that the wires are top-illuminated with transverse magnetic (TM, E-field along the wire) or transverse electric (TE, E-field normal to the wire) light. When the electric field is normal to the metal slit a strong plasmonic resonance can be excited in the slit. c) SEM image of a 90-nm-diameter Ge NW placed in a 150-nm-wide slit formed between two 150-nm-thick Ag pads. Scale bar is 200 nm. d) Simulated enhancement of the absorption in a Ge NW in a Ag slit as a function of the metal electrode thickness. The enhancement was measured with respect to a bare Ge NW of the same diameter. The simulation was performed at an excitation wavelength of 650 nm and for TE polarization. The dashed blue line represents an enhancement factor of 1 (i.e. no enhancement). e) and f) Distribution of magnetic field intensity H_z in the cross sectional plane of the device with a 150 nm or a 350nm Ag thickness respectively. Scale bar is 200nm.

II.6 Cathodoluminescence Characterization of Optical Antenna-emitters.

The successful realization of future, ultra-compact photonic devices will require the development of new techniques capable of correlating the nanostructural properties of materials and devices to their optical performance. In collaboration with Albert Polman's group at the FOM-Institute in the Netherlands, we have used utilize electron-beam based techniques that can simultaneously map the morphology and optical modes of plasmonic nanocavities and antennas at very high spatial resolution. An example structure that we pursued is a planar antenna structure that mimics the properties of a parabolic antenna (See Fig. 6).

Parabolic reflectors are well known in geometrical optics; they couple the emission of a point source at the parabolas' focus to a plane wave propagating parallel to parabola's axis, and vice versa. In a classical three-dimensional parabola the emitted light beam originates from the specular reflection of light over the entire parabola's surface. However, due to the special geometrical properties of a parabola, an array of individual scatterers placed in a parabolic arrangement will also generate a parallel beam of light in the far-field. In fact, a point source coupled to any two-dimensional sub-section of a paraboloidal surface will generate a wave preferentially propagating parallel to the paraboloid's axis. One special case of such a sub-section is the elliptical intersection of a paraboloid with a planar surface, with the paraboloid and the planar ellipse sharing a common focus. In such a geometry, a beam of light can be generated by exciting surface plasmon polaritons (SPPs) at an arbitrary location inside the planar ellipse followed by coherent scattering of the SPP to free-space photons via the edges of the area in the form of a collimated beam. The direction of the beam is only determined by the position of the source inside the ellipse and the ellipse's eccentricity. Figure 6a schematically shows this geometry.

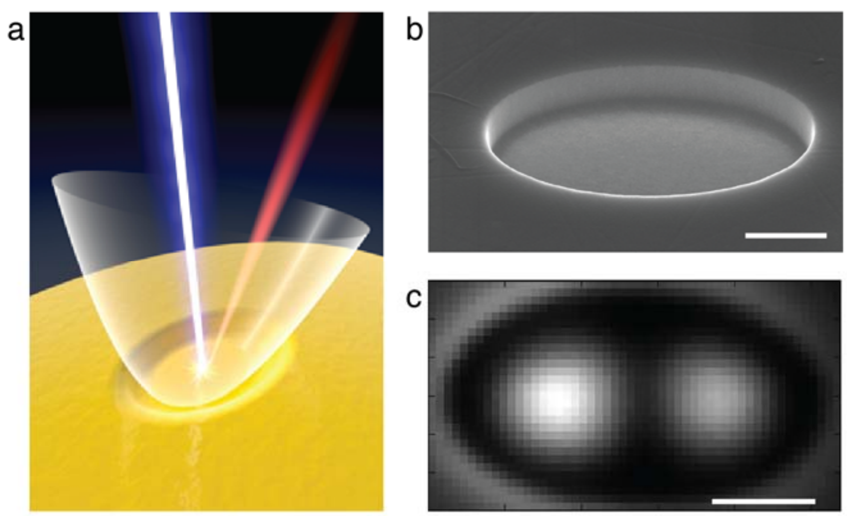

Figure 6: Elliptical cavity antenna design, realization, and operation. a. Schematic of the cross the section of a paraboloid with a planar surface, creating an ellipse. b. SEM image of elliptical arena taken at 52° off the surface normal. The scale bar is 500 nm. c. 30 keV cathodoluminescence image at a collection wavelength of 720 nm for a 1.0-μm long, 800-nm wide elliptical cavity. Scale bar is 250 nm. In a the incident electron beam is indicated in white/blue, the directional output beam in red.

We fabricated elliptical arenas using focused ion beam (FIB) milling into the surface of a single-crystalline Czochralski-grown Au(111) pellet that was mechanically polished to nanometer-scale roughness. A scanning electron microscopy (SEM) image of a characteristic ellipse is shown in Fig. 6b. Several different elliptical geometries were fabricated with major axes lengths ranging between 500 and 1600 nm, and eccentricities, defined as the ratio between the major axis length and the focus-to-focus distance, between 0 and 1. The depth of the elliptical cavity was also varied; typically a depth of 400 nm was used. The localized optical modes in these structures were determined using our newly developed angle-resolved cathodoluminescence imaging spectroscopy (ARCIS) technique. A 30 keV electron beam is raster-scanned over the surface and serves as a broad-band point source of surface plasmon polaritons. The radiation spectrum emitted by the antenna is collected by a half-paraboloidal mirror (focal length 0.5 mm) placed between the microscope's pole piece and the sample. In parallel, the angular distribution of the emitted light is recorded by collecting the light beam emanating from the collection paraboloid on a two-dimensional CCD camera. Figure 6c shows a cathodoluminescence (CL) image of a 1000×600 nm elliptical cavity recorded at a wavelength of 720 nm. The pixel size in the images of the smaller cavities is 10×10 nm, and it is 20×20 nm in the largest cavities. The two foci of the elliptical antenna are clearly resolved in the image, demonstrating the subwavelength resolution of the CL technique. As CL is a direct probe of the radiative component of the local density of optical states (LDOS), images such as in Fig. 6c provide a direct absolute measure of the radiation power of the antenna at any wavelength. This paper clearly showed the effective use of cathodoluminescence in the design of nanoscale optical sources and antennas. A paper on this topic was published in collaboration with Albert Polman's group in the journal Nano Letters ("The planar parabolic optical antenna," David Schoen, Toon Coenen, F Javier Garcia de Abajo, Mark L. Brongersma, Albert Polman, Nano letters 13, 188-93 (2013).

III. Personnel and Training Opportunities

III. 1. Personnel Supported

At Stanford University, this program supported research in the group of Prof. Mark L. Brongersma (PI). At different times, it funded work by two students Kevin Huang and Pengyu Fan as well two postdocs: Wenshan Cai and David Schoen. The researchers were together working on several projects aimed at the development of plasmonic nanocircuit elements.

III.2. Research Training of Students

The training of graduate students and postdoctoral researchers was a critical aspect of thius project. The sudden burst of activity in the field of plasmonics has led to hundreds of publications in the international literature and popular press. New conferences and symposia are devoted to just this topic (a number organized by the PIs). Major companies, such as Northrop Grumman, IBM, and Hewlet Packard now have active research efforts in this field.

> *….Hence, this is an excellent time for universities to train students to design, fabricate, and analyze nanophotonic and plasmonic devices and push the science and technology of these devices to new heights….*

IV. Dissemination of Research findings

IV.1.Publications, Books, and Presentations

The research from this program led to a total of 7 publications in refereed journals of which there were a number in very prestigious journals such as Nature Photonics, Nature Communications, and Science. The PI also contributed to two book chapters that incorporate material from this effort: Brongersma gave a total of 43 invited talks (including several keynotes) and presented 3 short courses at the CLEO conferences that used materials from this research effort. In the students funded by this effort presented a number of contributed talks at International conferences.

Publications in 2013

1. "Redesigning Photodetector Electrodes as an Optical Antenna," Pengyu Fan, Kevin C. Y. Huang, Linyou Cao, and Mark L. Brongersma, Nano Lett., 13, 392–396 (2013).
2. "The planar parabolic optical antenna," David Schoen, Toon Coenen, F Javier Garcia de Abajo, Mark L. Brongersma, Albert Polman, Nano letters 13, 188-93 (2013).

Publications in 2012

(1) "Electrical control of plasmonic Nanodevices," Wenshan Cai, Young Chul Jun, and Mark L. Brongersma, SPIE Newsroom. doi: 10.1117/2.1201112.004060 (2012).
(2) "An Invisible Metal-Semiconductor Photodetector," Pengyu Fan, Uday Chettiar, Linyou Cao, Farzaneh Afshinmanesh, Nader Engheta, and Mark L. Brongersma, Nature Photonics 6, 380–385 (2012).
(3) Book Chappter entitled: "Optical antennas for information technology and energy harvesting," Mark Brongersma, in "Optical Antenna Theory, Design and

Applications," Editors A. Alù, and N. Engheta, Cambridge University Press (2012)

Publications in 2011

(1) "Electrically Controlled Nonlinear Generation of Light with Plasmonics," Wenshan Cai, Alok P. Vasudev, Mark L. Brongersma, Science 333, 1720-1723 (2011).
(2) "Plasmonic beaming and active control over fluorescent emission," Young Chul Jun, Kevin C.Y. Huang, and Mark L. Brongersma, Nature Communications, 2, 283 (2011).
(3) "Power flow from a dipole emitter near an optical antenna," Kevin C. Y. Huang, Young Chul Jun, Min-Kyo Seo, and Mark L. Brongersma, Optics Express, 19, 19084-19092 (2011).

Publications in 2010

(1) Book Chapter entitled: "Applications: Nanophotonics and Plasmonics," E.L. Hu, M.L. Brongersma, A. Baca, Springer 2010, Chapter 9 of a WTEC (World Technology Evaluation Center) study on 'Nanotechnology Research Directions.

IV.2. Interactions and Transitions

This project has created a number of exciting opportunities for knowledge transfer in the first three years. The work on beaming and directing the emission from quantum emitters has help initiate a Navy STTR with Dr. Salah Khodja from Ultimara on active, plasmonic beam-steering devices. The work on integrated optical sources also attracted significant interest from Intel and resulted in a regular interaction with Bruce Block from Intel, Oregon. Knowledge transfer also occurred via individual interactions, presentations, and short courses.

IV.3. Honors and Awards

Brongersma was honored with the Raymond and Beverly Sackler Prize in the Physical Sciences for Physics for his work on plasmonics. He also became a Fellow of the American Physical Society in 2010 and a Fellow of the SPIE in 2011.